Catalytic Properties and Kinetic Mechanism of Human Recombinant Lys-9 Histone H3 Methyltransferase SUV39H1: Participation of the Chromodomain in Enzymatic Catalysis†

Hang Gyeong Chin,‡,§ Debasis Patnaik,‡,§ Pierre-Olivier Estève,‡ Steven E. Jacobsen,|| and Sriharsa Pradhan*,‡

New England Biolabs, 240 County Road, Ipswich, Massachusetts 01938, and Howard Hughes Medical Institute, University of California, Department of Molecular Cell and Developmental Biology, and Molecular Biology Institute, University of California, Los Angeles, California 90095

Received October 3, 2005; Revised Manuscript Received December 16, 2005

ABSTRACT: Histone H3 lysine 9 (H3K9) methylation is a major component of gene regulation and chromatin organization. SUV39H1 methylates H3K9 at the pericentric heterochromatin region and participates in the maintenance of genome stability. In this study, a recombinant purified SUV39H1 is used for substrate specificity and steady-state kinetic analysis with peptides representing the un- or dimethylated lysine 9 histone H3 tail or full-length human recombinant H3 (rH3). Recombinant SUV39H1 methylated its substrate via a nonprocessive mechanism. Binding of either peptide or AdoMet first to the enzyme made a catalytically competent binary complex. Product inhibition studies with SUV39H1 showed that *S*-adenosyl-L-homocysteine is a competitive inhibitor of *S*-adenosyl-L-methionine and a mixed inhibitor of substrate peptide. Similarly, the methylated peptide was a competitive inhibitor of the unmethylated peptide and a mixed inhibitor of AdoMet, suggesting a random mechanism in a bi-bi reaction for recombinant SUV39H1 in which either substrate can bind to the enzyme first and either product can release first. The turnover numbers (k_{cat}) for the H3 tail peptide and rH3 were comparable (12 and 8 h^{-1}, respectively) compared to the value of 1.5 h^{-1} for an identical dimethylated lysine 9 H3 tail peptide. The Michaelis constant for the methylated peptide (K_m^{pep}) was 13-fold lower compared to that of the unmethylated peptide. The Michaelis constants for AdoMet (K_m^{AdoMet}) were 12 and 6 μM for the unmethylated peptide substrate and rH3, respectively. A reduction in the level of methylation was observed at high concentrations of rH3, implying substrate inhibition. Deletion of the chromodomain or point mutation of the conserved amino acids, W64A or W67A, of SUV39H1 impaired enzyme activity despite the presence of an intact catalytic SET domain. Thus, SUV39H1 utilizes both the chromodomain and the SET domain for catalysis.

Histone modifications play a major role in the control of gene expression in the native chromatin context in eukaryotes. In eukaryotes, chromatin is formed by association of 146 bp of DNA and a histone octamer consisting of two of each of the following histones: H2A, H2B, H3, and H4 (*1*). The amino termini of the histone molecules protrude away from the nucleosome core and thus are amenable to several forms of posttranslational modifications such as acetylation, methylation, phosphorylation, ubiquitination, and ADP ribosylation (*2*, *3*). Acetylation of specific Lys (K) and methylation of Arg (R) residues are shown to be involved in transcriptional activation (*4*−*6*), although methylation of Lys-9 and -27 residues is implicated in gene repression (*7*−*9*). Similarly, phosphorylation of Ser residues is involved in early gene activation and chromatin condensation (*10*−*12*). In histone H3 (H3), several Lys residues are methylated. Among them, the most notable are K4, K9, K27, K36, and K79. Transcriptional regulation in eukaryotic genes often involves K4 and K9 methylation. K4 trimethylation is observed in fully activated promoters (*13*, *14*), whereas K4 dimethylation correlated with basal gene expression (*14*). This observation suggests promoter activation as a function of the presence on a particular promoter of H3K4 methylated to various degrees. In contrast to H3K4 methylation, H3K9 methylation is found mainly in silent chromatin. Many neural genes are transcriptionally repressed outside the nervous system via highly enriched H3K9 dimethylated molecules (*15*). A similar mechanism is also found in postinduction repression of the interferon β gene in osteosarcoma cell line U2OS through accumulation of H3K9 dimethylated molecules (*16*). Dosage compensation in female mammals involves inactivation of one X chromosome (Xi) (*17*), and this inactivation is shown to be associated with H3K9 methylation (*18*).

Histone methyltransferases often possess a SET domain region (*21*, *22*) and, in some cases, also contain a chromodomain (*19*, *20*). The SET domain includes the catalytic region of the protein, and mutation of conserved amino acids in this region often abolishes its catalytic activity (*23*, *24*). Several different histone methyltransferases can perform

† S.E.J. was supported by NIH Grant GM60398.

* To whom correspondence should be addressed. Telephone: (978) 380-7227. Fax: (978) 921-1350. E-mail: pradhan@neb.com.

‡ New England Biolabs.

§ These authors contributed equally to this work.

|| University of California.

10.1021/bi051997r CCC: $33.50
Published on Web 02/15/2006

H3K9 methylation, including *Drosophila*, SU(VAR)3-9, Clr4 of *Schizosaccharomyces pombe*, murine Suv39h1, Suv39h2, and G9a, and human SUV39H1 and SUV39H2 (*7*, *23*, *25*, *26*). Methylation of H3K9 creates a high-affinity binding site for the chromodomain of heterochromatic protein 1 (HP1) (*27*). Genetic deletion of SUV39H1 or SUV39H2 leads to a reduction of the level of global K9 trimethylation in the pericentric heterochromatic regions (*28*, *29*), and G9a genetic deletion results in a reduction of the level of global K9 dimethylation (*7*). Null mutants of either G9a or SUV39H1 displayed impaired viability and a reduction of the level of global H3K9 methylation from either euchromatic or heterochromatic regions, suggesting a unique function of these enzymes during growth and development (*24*, *30*).

The mechanism of K9 methylation in *Neurospora crassa*, DIM-5 (*31*, *32*), human SET7/9 (*33*, *34*), and *Drosophila* SU(VAR)3-9 (*35*) and, more recently, the kinetic mechanism of murine G9a (*36*) have been studied. Structural and mutational studies with DIM-5 revealed no similarity with previously characterized AdoMet-dependent methyltransferases, but DIM-5 did contain a new triangular Zn_3Cys_9 zinc cluster in the pre-SET region and an AdoMet binding site at the SET domain that is essential for catalysis (*31*). The ternary structure of DIM-5 with *S*-adenosyl-L-homocysteine and the substrate H3 peptide demonstrated a surface groove that binds the methylated region of the H3 peptide along with the post-SET region, contributing to both cofactor and peptide binding via conserved cysteine residues (*32*). The cofactor binding site in DIM-5 is an open concave pocket in a folded conformation as observed previously for Rubisco methyltransferase (*37*) and SET7/9 (*22*, *33*, *38*). This concave pocket is larger than one cofactor binding site and possibly associated with release of reaction product AdoHcy with AdoMet without release of the peptide, thus contributing to the processivity of the enzyme without the release of the substrate. H3K9 methyltransferase, G9a, can perform trimethylation of the target Lys-9 without being released from the peptide substrate (*36*). The solution structure of Lys-27 methyltransferase, vSET, revealed a butterfly-shaped head-to-head symmetric dimer. Each dimer has two domains, and the flexible C-terminal segment of vSET is believed to be involved in AdoMet binding and/or substrate recognition for catalysis (*39*). Another example of homodimer formation is observed in *Drosophila* SU(VAR)3-9 histone methyltransferase. The amino terminus of the enzyme participates in this interaction, resulting in an increase in histone methyltransferase activity (*35*). Recently, two different euchromatic histone methyltransferases, Eu-HMTase1 and G9a, were shown to form heterodimers in a variety of cell types. This heterodimer formation is dependent on the SET domain and is hypothesized to be involved in enzymatic methylation cooperation in vivo (*40*).

Although histone methyltransferases can cooperate functionally, they can also direct different degrees of methylation to different chromatin domains (*28*, *29*). Using antibodies specific for mono-, di-, and trimethylated Lys-9 of histone H3, it has been demonstrated that G9a is a mono- and dimethylase and SUV39H1 is a trimethylase. The in vitro methylation reaction carried out by G9a demonstrates it is capable of mono-, di-, and trimethylation of Lys-9 (*36*, *41*). Furthermore, immunocytochemical experiments with transfected cells demonstrate the presence of SUV39H1 at heterochromatin and G9a at euchromatin. However, little is known about the reaction mechanism and functional association of the chromodomain in the methylation reaction mediated by SUV39H1. To elucidate the methyltransferase properties of SUV39H1, we have performed preincubation studies and examined the reaction mechanisms, including order of substrate binding and product inhibition studies. Steady-state kinetic analysis with a variety of peptide substrates mimicking amino-terminal tails of histone H3 as well as recombinant full-length histone H3 is reported here. We have also generated a series of chromodomain mutants, purified the enzymes, and studied their catalytic properties. We propose that the chromodomain contributes to the catalytic mechanism of SUV39H1.

MATERIALS AND METHODS

SUV39H1 Fusion Constructs and Baculovirus Transfer Vector. The full-length SUV39H1 cDNA clone was obtained from ATCC (MGC 10376, GenBank accession number BC006238). This plasmid contains the full-length human cDNA based on the previously published sequence (*23*). A PCR with the 3′ end of the cDNA was used to incorporate an EcoRI restriction endonuclease site in place of the stop codon of the cDNA and to provide the optimal amino acids for intein tag cleavage (sense primer, 5′-TCGCGACATATG-GCGGAAAATTTAAAAGGCTGC-3′; and antisense primer, 5′-ACGGAATTCGAAGAGGTATTTGCGGCAGGACTC-3′). The restriction sites are underlined. The addition of an EcoRI site resulted in addition of Glu and Phe to the last amino acid, Thr, of SUV39H1. The PCR product was cloned in pVIC using NdeI and EcoRI downstream of the polyhedrin promoter. In pVICSUV39H1, the cDNA remained in frame with the intein chitin-binding domain of the pVIC1 transfer vector. The ligated junctions in the final pVICSUV39H1 construct were verified by DNA sequencing.

For the cloning of SUV39H1 in pMALc2X (NEB), the following PCR primers were used: sense primer, 5′-CGGAATTCCATGGCGGAAAATTTAAAAGGCTG-C-3′; and antisense primer, 5′-ACGCGTCGACCTAGAAGA-GGTATTTGCGGCAGGA-3′. The PCR product was digested with SalI and ligated with the pMALc2X vector digested with XmnI and SalI.

Generation of Chromodomain Deletions and Point Mutant SUV39H1s. Chromodomain deletion MBP fusion Δ80SUV-39H1 was generated by PCR amplification with forward primer SUVfp241A (CGGAATTCATGAAGTGTGTGCG-TATCCTCAA) and reverse primer SUV39H1rp (ACGCGTC-GACCTAGAAGAGGTATTTGCGGCAGGA). The PCR product was cloned into pMALc2x using EcoRI and SalI sites. MBP fusion ΔCDSUV39H1 was made using two PCR products. The PCR product for SUV39H1(1−42) was amplified using forward primer SUV39fpA (GCGAAT-TCATGGCGGAAAATTTAAAAGGC) and reverse primer SUVrp126 (GTCATAGAGGTTCCTCTTAGAGAT). PCR product SUV39H1(81−end) was amplified using forward primer SUVfp241 (AAGTGTGTGCGTATCCTCAAGCA) and reverse primer SUV39H1rp (ACGCGTCGACCTA-GAAGAGGTATTTGCGGCAGGA). PCR-amplified products of SUV39H1(1−42) and SUV39H1(81−end) were digested with EcoRI and SalI, respectively, and purified using a spin column. The digested inserts were treated with T4

polynucleotide kinase for 30 min at 37 °C and ligated to pMALc2X at EcoRI and SalI sites. Correct clones were confirmed by restriction digestion and sequencing.

Insect Cell Culture, Viral Transfection, and Recombinant SUV39H1 Expression. A pupal ovarian cell line (Sf9, Invitrogen) from the worm *Spodoptera frugiperda* was used for cotransfection and expression of SUV39H1 as described previously (*36*) with the following modifications. Sf9 cells were maintained as a suspension culture in TNM-FH medium (JRH Biosciences) supplemented with 10% (v/v) fetal calf serum and an antibiotic/antimycotic solution at a final concentration of 5 units of penicillin, 50 μg of streptomycin, and 0.125 μg of amphotericin B per milliliter at 27 °C on a Bellco stirring platform at 70 rpm. Cotransfection of a monolayer of Sf9 insect cells was carried out using BaculoGold DNA, a modified linearized *Autographa californica* nuclear polyhedrosis virus (AcNPV) DNA (BD Pharmingen), and transfer vector pVICSUV39H1. Five days after transfection, the supernatant was harvested (P1 viral stock) and amplified two more times (P2 and P3 amplification) to reach a viral titer above 2×10^8 mL^{-1} as estimated by the agarose overlay technique (*42*). Recombinant viruses from the P3 viral stock were used for test expression by infecting 2×10^6 Sf9 cells at different multiplicities of infection (MOI) in a 60 mm Petri dish. Forty-eight hours postinfection, the cell extracts were checked for histone H3 methyltransferase activity and for fusion protein expression by Western blot analysis using an anti-CBD monoclonal antibody (New England Biolabs). For routine protein expression, Sf9 cells were grown in spinner culture flasks. Sf9 cells at a density of 1.1×10^6 cells/mL were infected at a multiplicity of infection between 6 and 10. The cells were kept at 27 °C at 60 rpm and harvested 48 h postinfection after a final wash with 1× PBS.

Recombinant SUV39H1 Purification. For protein purification, infected cells (5.6×10^8) were resuspended in 15 mL of buffer H [50 mM Tris-HCl (pH 8.0), 5 mM $MgCl_2$, protease inhibitor cocktail containing 4-(2-aminoethyl)-benzenesulfonyl fluoride, pepstatin A, E64, bestatin, leupeptin, and aprotinin (Sigma), 0.2% (v/v)/mL cell extract, 7 μg/mL PMSF, and 500 mM NaCl]. Sample processing and protein purification steps were similar to those for G9a described previously (*36*). The target protein was allowed to be cleaved from the intein tag by overnight incubation at 4 °C. Recombinant SUV39H1 was eluted with buffer H containing 50 mM DTT and dialyzed against buffer H supplemented with 0.2% (v/v) protease inhibitor cocktail (Sigma), 7 μg/mL PMSF, 150 mM NaCl, 50% (v/v) glycerol, and 4 mM DTT. The purified protein was stored at −20 °C. The purity of the protein was checked by SDS−PAGE (4 to 20% Tris−glycine−SDS gradient gel) and quantitated using a Bradford assay with bovine serum albumin (BSA) as a standard.

MBP−SUV39H1 fusions were purified by following the manufacturer's recommendation (NEB). The cells were resuspended in 50 mL of MBP column buffer [50 mM Tris-HCl (pH 8.0), 200 mM NaCl, 5 mM $MgCl_2$, 2 mM DTT with 0.2% protease inhibitor cocktail, and 7 μg/mL PMSF]. Cell extract was applied onto amylose resin washed with 60 volumes of column buffer, and the fusion protein was eluted by adding 10 mL of MBP elution buffer (column buffer supplemented with 10 mM maltose).

Histone Methyltransferase Assay for Initial Velocities. Methyltransferase assays were carried out at 25 °C for 3 min in duplicate with a total volume of 25 μL of reaction mix. A typical reaction mixture contained a mixture of *S*-adenosyl-L-[*methyl*-^{3}H]methionine (AdoMet) (specific activity of 15 Ci/mmol, Amersham Pharmacia), substrate peptide, and SUV39H1 enzyme in assay buffer [50 mM Tris-HCl (pH 8.5), 5 mM $MgCl_2$, 4 mM DTT, and 7 μg/mL PMSF]. For kinetic analysis, the AdoMet stock concentration and the K9 peptide concentration were calculated from the molecular weight. For higher concentrations of AdoMet, both tritiated and cold AdoMet (NEB) were added. In the Michaelis−Menten plots, the concentrations of the peptide and AdoMet were varied. Recombinant wild-type (WT) histone H3 was used as a substrate in place of WT-H3 peptide for the determination of kinetic constants. The methyltransferase reactions were stopped by transferring the reaction tubes to an ethanol/dry ice bath or spotted directly onto P81 paper circles (Whatman). These circles were washed sequentially three times (5 mL/circle) with 0.2 M cold ammonium bicarbonate and dried at 65 °C for 10 min. SafeScint scintillation cocktail (2.5 mL, American Bioanalytical) was added to each, and the level of tritium incorporation was measured. All methylation values were corrected for nonspecific binding of *S*-adenosyl-L-[*methyl*-^{3}H]methionine to the processed filter. Background calculations were measured in the absence of enzyme or substrate at time zero. To calculate the counting efficiency, internal tritium standards were used. The efficiency of [^{3}H]DNA measurement was ∼55%, and all calculations were corrected accordingly. Data were plotted by regression analysis using GraphPad PRISM 4c (GraphPad Software Inc.).

Processivity and Preincubation Studies. A master mix (600 μL) containing 2.2 μM biotin-conjugated histone H3 tail peptide (WT H3) and 25 nM SUV39H1 was incubated at room temperature for 6 min to facilitate formation of the SUV39H1−peptide binary complex followed by addition of 25 μM AdoMet. After 3 min, 300 μL was removed and mixed with 44 μM WT-H3 non-biotin tail peptide (no biotin). Aliquots (25 μL) were withdrawn at 3 min intervals up to 15 min, and the reaction was stopped with 5 μL of 20% (v/v) TFA. To the reaction mix were added 50 μL of 1× PBS and 25 μL of streptavidin magnetic beads (0.1 mg, NEB). The captured peptides were washed with 3×1 mL of 0.2 M cold ammonium bicarbonate, air-dried, and finally dissolved in 50 μL of 0.2 M ammonium bicarbonate and transferred to the scintillation vial. SafeScint scintillation cocktail (2.5 mL) was added and mixed before radioactive measurement.

Preincubation experiments were carried out by incubating 25 nM SUV39H1 with either 25 μM *S*-adenosyl-L-[*methyl*-^{3}H]methionine or 2.2 μM WT-H3 for 10 min. The reaction was started by adding the missing reactant, i.e., peptide (final concentration of 2.2 μM), in the first reaction mix and *S*-adenosyl-L-[*methyl*-^{3}H]methionine (25 μM) to the second one. Aliquots (10 μL) were withdrawn at each 5 min interval up to 30 min and spotted directly on P81 and processed as described above.

Peptide Substrates for Methylation Analysis. Peptides were synthesized at New England Biolabs and purified by HPLC, and intactness and purity were checked with mass spectroscopy. Peptides used in this study are listed in Table 1. For

Table 1: Substrates and Methylated Peptides Used in Kinetic Analysis of Recombinant SUV39H1[a]

sequence	name
CARTKQTARKSTGGKAPRK-BT	WT-H3
CARTKQTAR(2-meK)STGGKAPRK-BT	WT-H3(K9-dime)
CARTAQTARKSTGGY-BT	K4AK9
CARTAQTAR(3-meK)STGGY-BT	K4AK9-trime

[a] Abbreviations: BT, biotin; 2-meK, dimethyllysine; 3-meK, trimethyllysine.

kinetic analysis, all peptides were dissolved in MilliQ sterilized water and kept frozen at −20 °C before they were used.

Enzyme Assay for Initial Velocities in the Absence of Products and Data Analysis. All initial velocity studies were performed under identical conditions as described for the histone H3 methyltransferase assay. For initial velocity studies with WT-H3 and WT-H3(K9-dime), the peptides (0.07−6.6 μM) were incubated with 25 nM recombinant SUV39H1 and 25 μM *S*-adenosyl-L-[*methyl*-^{3}H]methionine. With rH3, the substrate concentration varied from 0.02 to 3.3 μM. The extent of product formation was kept below 5% of the substrate to prevent the inhibition effect. The amount of product that formed was measured in counts per minute (cpm). The nanomolar product formed ([^{3}H]CH_3 group transfer) (*N*) present at the end of the reaction was calculated with the relation $N = (Y - B)/(EF)$, where *Y* is the value from the cpm experiment, *B* is the cpm blank, *E* is the efficiency (0.55), and *F* is cpm per nanomolar free AdoMet. The amount of product formed per minute was obtained as *N*/*T*, where *T* is the time of the reaction. The nanomolar per minute value was fitted to a one-site binding (hyperbola) equation.

$$v = (V_{max}[S])/(K_m + [S]) \quad (1)$$

This describes binding of a substrate or ligand to an enzyme that follows the law of mass action. V_{max} is the maximal velocity, and K_m is the concentration of substrate needed to reach the half-maximal velocity. All data points were analyzed by nonlinear regression. From V_{max}, the turnover number (k_{cat}) was calculated.

$$k_{cat} = V_{max}/[E_t]$$

where $[E_t]$ is the total enzyme concentration. For double-reciprocal plots, the initial velocity $1/v$ was obtained as $[E_t] \times T/N$. Data points were collected in duplicate, plotted on Lineweaver−Burk double-reciprocal plots, and fitted to weighted linear regression. The families of linear regression plots give a preliminary clue about the nature of the reaction mechanism. These plots essentially gave two independent variables, namely, the reciprocals of the apparent V_{max} (V_{max}^{app}), given by the *y*-axis intercepts, and the ratio of the Michaelis constant (K_m) (plus the dissociation constant) for the variable substrate to V_{max}^{app}, given by the slope. By replotting the intercepts and slopes that were obtained, one would also determine the true V_{max} and K_m for a substrate. The equations used for fitting the data points and for obtaining the kinetic constants (V_{max}, K_m^{pep}, and K_m^{AdoMet}) are reported elsewhere (*43*). These figures represent estimated values.

Enzyme Assay for Initial Velocities in the Presence of Products and Data Analysis. Initial velocity studies in the presence of products were performed to distinguish the reaction mechanism. SUV39H1 has two products at the end of the reaction: one AdoHcy (*S*-adenosyl-L-homocysteine) and trimethylated histone H3 or peptides mimicking the histone H3 tail. AdoHcy (Sigma) was dissolved in 10 N HCl and diluted with MilliQ water to 100 μM. The methylated peptide was dissolved in MilliQ water. Assays were performed as described previously, with the exception of addition of a fixed amount of end products. In the experiments with AdoHcy, the concentration ranges of the reactants were 0.25−1.1 μM for WT-H3, 2−25 μM for AdoMet, and 0−20 μM for AdoHcy. For the assay with the trimethylated peptide, the concentration ranges of the reactants were 0.22−6.6 μM for WT-H3, 0−3 μM for the trimethylated peptide, and 2−25 μM for AdoMet. The sequence of the trimethylated peptide was CARTKQTAR(3-meK)STGGKAPRKQLATKAAR(3-meK)SAPA. The data obtained from inhibition studies were fitted to the following equations.

competitive inhibition:

$$v = (V_{max}[S])/[S] + K_m(1 + [I]/K_i) \quad (2)$$

mixed inhibition:

$$v = (V_{max}[S])/[S](1 + [I]/\alpha K_i) + K_m(1 + [I]/K_i) \quad (3)$$

where v is the initial velocity, V_{max} the velocity maximum, K_m the Michaelis constant, K_i the inhibition constant, and αK_i the inhibition constant (the factor α reflects the effect of the inhibitor on the affinity of the enzyme for its substrate and the effect of the substrate on the affinity of the enzyme for the inhibitor).

RESULTS

Expression and Preliminary Characterization of Recombinant SUV39H1. Cotransfection of the pVICSUV39H1 transfer vector along with linear DNA of *A. californica* nuclear polyhedrosis virus (AcNPV) on a monolayer of Sf9 cells resulted in generation of recombinant SUV39H1 baculovirus as determined by Western blot analysis of Sf9 cell extracts that were inoculated with a P1 viral stock for 48 h. For protein expression, the P3 viral stock at a multiplicity of infection (MOI) of 8 for 48 h at 27 °C was found to be optimal. The recombinant protein was soluble and purified on a chitin affinity matrix after DTT cleavage. The only other contaminant in the enzyme preparation was the viral chitinase due to its strong affinity for the chitin matrix (Figure 1A). The enzyme was dialyzed and kept at −20 °C for several weeks without any appreciable loss of activity. However, DTT appeared to be an essential component for enzyme stabilization. We also examined if the residual chitinase in the enzyme preparation had any effect on enzyme activity by incubating the purified chitinase enzyme in the presence of tritiated AdoMet and measuring the level of radioactive incorporation with respect to time. A time course of reaction revealed no detectable amount of methyltransferase activity in the purified enzyme (data not shown). This recombinant full-length SUV39H1 was used in all kinetic studies reported here. We also produced MBP-fused SUV39H1 (MBP−SUV39H1) which was purified on

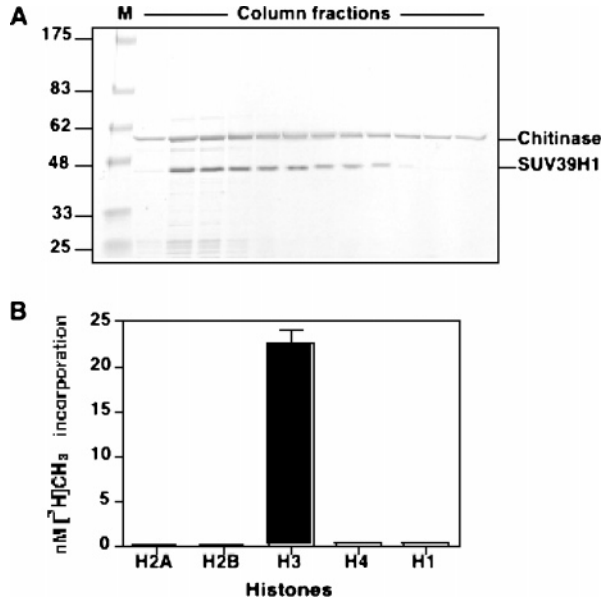

FIGURE 1: Purification and methylation specificity of recombinant SUV39H1 on histones. (A) Affinity column purification of recombinant human SUV39H1 on a chitin matrix. Eluted protein samples from a chitin column were separated via SDS−PAGE and visualized by Coomassie staining. Lane M contained prestained molecular mass markers from NEB. The mass of each band is indicated at the left, and column fractions are at the top. Coeluted host cellular chitinase is also denoted. (B) Histone substrate specificity of recombinant baculovirus-expressed SUV39H1. A 30 min methylation reaction was performed with 0.55 μM recombinant histone and 25 nM SUV39H1 in the presence of AdoMet. The recombinant histones that were used are indicated at the bottom, and nanomolar concentrations of methylation are given on the *y*-axis.

an amylose affinity column (Figure 10B). This was utilized for the deletion studies reported in Figure 10.

The substrate specificity of baculovirus-produced SUV39H1 was compared with that of G9a by incubating either SUV39H1 or G9a with various recombinant human histone molecules. Recombinant baculovirus-produced SUV39H1 methylated histone H3 exclusively (Figure 1B), although G9a methylated histone H3 and, to a lesser extent, histone H1 (data not shown). Thus, SUV39H1 is an exclusive histone H3 specific methyltransferase. We obtained similar results with the MBP-fused SUV39H1 (data not shown).

Recombinant baculovirus-produced SUV39H1 was assayed for its optimal pH, temperature, NaCl concentration, and substrate specificity. The methyltransferase reaction conditions were found to be strongly dependent on alkaline pH. The enzyme activity was almost undetectable at pH 7, but a surge in the level of methyl transfer was observed from pH 7.4 to 8.5 (Figure 2A). The enzyme is most active at 25 °C and loses its activity significantly at 37 °C (Figure 2B). SUV39H1 is sensitive to the presence of salt in the reaction since 200 mM NaCl in the reaction completely abolished its activity (Figure 2C). Synthetic peptide substrates corresponding to the amino-terminal tail of histone H3 (Table 1) were used to determine the relationship between substrate length and enzyme activity. WT-H3 containing amino acids 1−17 of histone H3 was methylated well but not a peptide containing amino acids 1−13 (Figure 2D), suggesting substrate length is a critical parameter for enzymatic catalysis.

Linearity of the Methylation Reaction by Recombinant SUV39H1. To determine the linearity of the Lys-9 methylation reaction catalyzed by SUV39H1, a fixed concentration of enzyme was incubated with a fixed amount of WT-H3 substrate and three different concentrations of AdoMet, and 10 μL of the reaction mix was withdrawn at the 5 min time interval for quantitative estimation of methylation. At all three concentrations of AdoMet (1, 5, and 25 μM), the reaction essentially remained linear up to the first 40 min (Figure 3A). A slight decrease in the rate of the reaction was observed after 40 min, possibly due to rapid accumula-

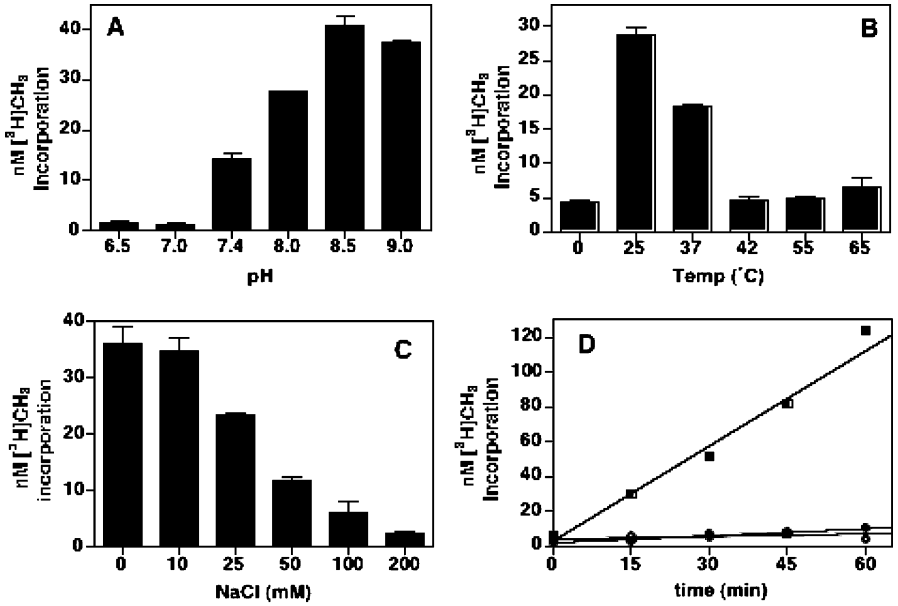

FIGURE 2: Reaction conditions for optimization of recombinant SUV39H1. (A) The histone methylation reaction with recombinant full-length SUV39H1 at various pH values is shown. Indicated at the bottom are pH, and nanomolar concentrations of methyl group incorporation are given on the *y*-axis. (B) Effect of temperature on histone H3 methylation catalyzed by recombinant SUV39H1. The incubation temperature of the reaction is given at the bottom. (C) Effect of NaCl on histone H3 methylation catalyzed by recombinant SUV39H1. The final NaCl concentration in the reaction is given at the bottom. (D) Velocity of the reaction with peptides used as a substrate for recombinant SUV39H1 methylation studies. Methyl group incorporation as a function of time with WT-H3 (■), WT-H3(1−13) (●), and K4AK9 (○) is shown. A list of peptides is given in Table 1. All these reactions were performed in duplicate with full-length baculovirus-expressed SUV39H1.

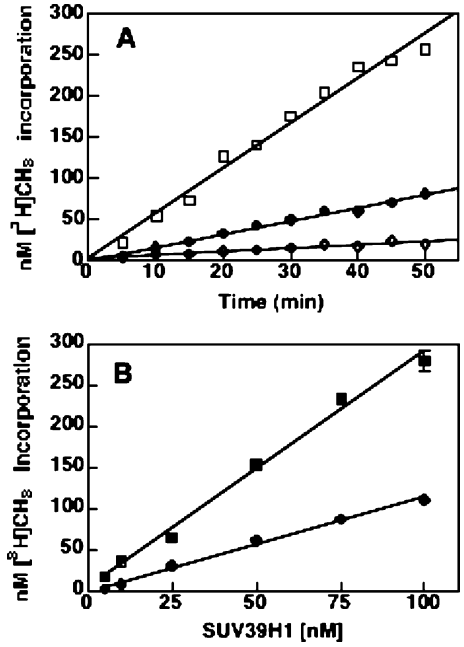

FIGURE 3: Linearity of the methylation reaction catalyzed by recombinant SUV39H1. (A) Linearity of the reaction as a function of time with three different concentrations of AdoMet: 1 (○), 5 (●), and 25 μM (□). The reaction mixture contained 5 μM WT-H3 substrate, 25 nM full-length SUV39H1, and AdoMet and was incubated at 25 °C; 10 μL of reaction mix was spotted in duplicate on P81 at fixed time intervals and processed as described in Materials and Methods. The mean values of radioactive incorporation are plotted as a function of time. Linear regression of methyl group incorporation is shown for all three concentrations of AdoMet. (B) Linearity of the methyl group transfer as a function of enzyme concentration. Duplicate reaction mixtures (25 μL) containing 5 μM WT-H3 and 5 (●) or 25 μM (■) tritiated AdoMet and an increasing concentration of recombinant SUV39H1 (5, 10, 25, 50, 75, and 100 nM) were incubated for 30 min at room temperature, and 10 μL of each reaction mixture was spotted and processed.

tion of product AdoHcy or methylated peptide. From these data, we chose an optimal and convenient reaction time of 30 min. A similar set of reactions was performed to determine the linearity of the reaction with respect to enzyme concentration at two different cofactor concentrations and a fixed amount of WT-H3 substrate peptide. In a 30 min reaction period, with 6 or 25 μM AdoMet, and between 5 and 100 nM enzyme, the enzymatic reaction remained essentially linear (Figure 3B). For the remaining experiments, we utilized 25 nM enzyme and a 30 min incubation at room temperature.

SUV39H1 Methylates Lys-9 in a Nonprocessive Manner. The amino group of a target lysine is capable of accepting three methyl groups, and SUV39H1 seems to be responsible for trimethylation of H3K9 in vivo, because loss-of-function SUVH39 mutants exhibit losses in the level of trimethylation in heterochromatin (*28*, *29*, *44*). To determine if SUV39H1 can methylate in a processive or repeated hit manner like that of the H3K9 methyltransferase G9a (*36*), we incubated the biotin-tagged WT-H3 peptide in the presence of a limiting amount of enzyme and an excess of tritiated AdoMet. We preincubated SUV39H1 with peptide for 6 min to promote forward binary complex formation. This complex was then made catalytically competent via addition of AdoMet and incubation for an additional 3 min. Following the second

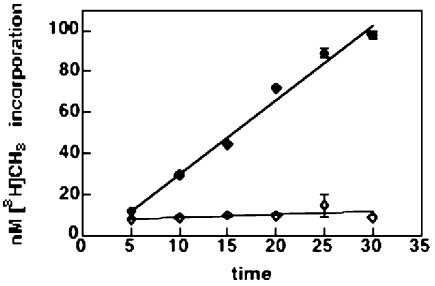

FIGURE 4: Nonprocessive methylation catalyzed by recombinant SUV39H1. Methyl group incorporation after the enzyme was preincubated at 25 °C with the WT-H3 peptide followed by tritiated AdoMet to start the reaction. Three minutes after the start of the reaction, the mixture was divided into two sets and one set was chased with WT-H3-nonbiotinylated excess peptide (○) or allowed to proceed without chase (●), as described in Materials and Methods. The reaction was monitored at 5 min time intervals by processing 25 μL of the reaction mixture in duplicate.

incubation, the reaction mixture was split in two and one-half was combined with a 20-fold excess of non-biotin-tagged peptide substrate. Reaction aliquots withdrawn at 5 min intervals were checked for methylation by capturing the biotinylated−methylated peptides via streptavidin magnetic beads and the unbound fraction by spotting directly on P81. If SUV39H1 acts in a repeated hit-type mechanism, it would dissociate from the substrate molecule after each round of methylation and would reassociate in the next round of catalysis. If, on the other hand, SUVH39H1 works in a processive manner, then dilution with a competitor peptide should not totally inhibit further methylation. We found that, in the presence of a 20-fold excess of nonbiotinylated peptide, the extent of the methylation reaction did not increase, but in the absence of nonbiotinylated competitor, rapid additional H3K9 methylation was observed (Figure 4). Furthermore, the unbound fractions with a 20-fold excess of nonbiotinylated peptide displayed a gradual increase in the level of methylation (data not shown). This suggests a repeated hit mechanism of methylation in which each cycle of methylation by SUV39H1 can load one methyl group onto the target lysine.

Preincubation Studies with Recombinant SUV39H1. A preincubation study can be used to demonstrate the catalytic competence of enzyme−substrate complexes in a reaction, particularly when the enzyme utilizes two different substrates (bisubstrate). Either of the substrates (AdoMet or peptide) can bind to the enzyme and make a catalytically competent enzyme−substrate complex (SUV39H1−AdoMet or SUV39-H1−peptide), as observed in the bi-bi random mechanism of enzymatic reaction (Figure 5A), or only one substrate can make a catalytically competent binary complex and the other follows to make the ternary complex as often seen in bi-bi sequential ordered mechanisms. In a bi-bi random enzymatic reaction mechanism, either of the products can release first, in contrast to the sequential mechanism in which product release is ordered. To study the catalytically competent enzyme−substrate complexes for SUV39H1, either WT-H3 peptide or AdoMet was incubated first with the enzyme followed by addition of the other substrate to form a ternary complex. The enzymatic catalysis was monitored at every 5 min interval, up to 30 min, by spotting 10 μL directly onto P81. The results are presented in Figure 5B, demonstrating that neither of the substrates has any profound impact on

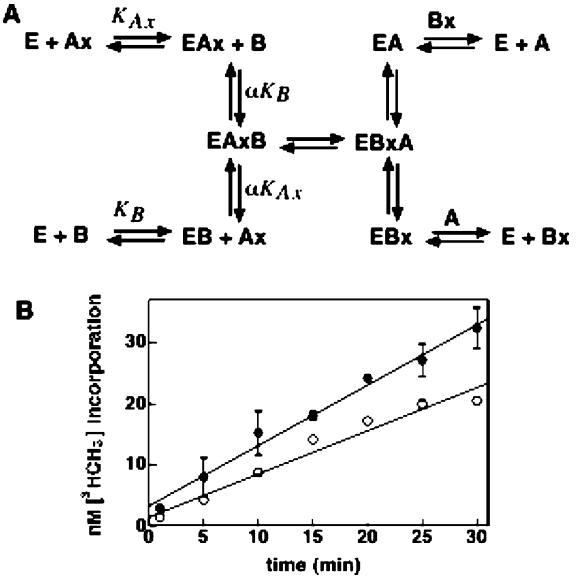

FIGURE 5: Reaction mechanism and preincubation studies with recombinant SUV39H1. (A) Bi-bi random mechanism of the enzyme reaction catalyzed by recombinant SUV39H1. E (SUV39H1), Ax or AdoMet (x being a methyl group), *B* (unmethylated peptide), A (AdoHcy), and Bx (methylated peptide) are shown. Binary (EAx, EB, EBx, and EA) and ternary (EAxB and EBxA) complexes are shown. The binding of AdoMet to free SUV39H1 is described by the dissociation constant K_{Ax}. Likewise, binding of SUV39H1 to the unmethylated peptide is described by K_B. Binding of AdoMet to the preformed SUV39H1−peptide binary complex is described by the constant αK_{Ax}. Similarly, binding of the SUV39H1−AdoMet complex to the unmethylated peptide is described by the constant αK_B. (B) Preincubation of recombinant SUV39H1, AdoMet, and peptide was performed as described in Materials and Methods. Methylation in the presence of a preformed SUV39H1−AdoMet binary complex (peptide added second) is shown with filled circles. Similarly, a preformed SUV39H1−peptide binary complex (AdoMet added second) is shown with empty circles. Ten microliters of the reaction mixture was spotted in each 5 min time interval, and the extent of methyl group incorporation was measured.

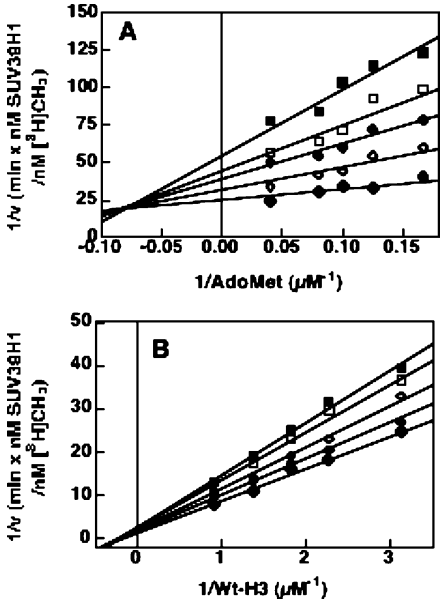

FIGURE 6: Double-reciprocal plots of the initial velocity vs substrate concentration for recombinant SUV39H1. (A) Double-reciprocal plots for increasing fixed peptide (WT-H3) concentrations of 0.32 (■), 0.44 (□), 0.55 (●), 0.726 (○), and 1.1 μM (◆) and variable AdoMet concentrations. Linear regression was performed, and $1/v$ is plotted vs 1/[AdoMet]. (B) Double-reciprocal plots for increasing fixed AdoMet concentrations of 6 (■), 8 (□), 10 (○), 12.5 (●), and 25 μM (◆) and variable peptide (WT-H3) concentrations. Linear regression was performed, and $1/v$ is plotted vs 1/[WT-H3].

the enzyme-catalyzed reaction since the rate of the reaction remained similar in both sets of experiments, suggesting SUV39H1 may have a random bi-bi mechanism of reaction (Figure 5A).

Initial Velocity Studies with Variable AdoMet and Peptide. Initial velocity experiments enable the determination of kinetic constants and provide insights into the kinetic mechanism of a reaction. A thorough understanding of the mechanism of SUV39H1 is critical in understanding gene silencing, genome stability, and heterochromatin formation. In the following experiments, the WT-H3 substrate was methylated at less than 5% of the acceptor methylation sites on Lys-9 with recombinant SUV39H1. We assumed that this small amount of product would not have any impact on catalysis. We plotted methyltransferase activity with the extent of methylation as a function of peptide or AdoMet as variable substrates. For a bisubstrate enzyme, such as SUV39H1, the double-reciprocal plots generally give linear responses when the reciprocal of velocity ($1/v$) is plotted as a function of the reciprocal substrate concentration ($1/s$). The plot of the reciprocal of velocity versus the reciprocal of substrate concentration gave a series of lines that were linear, whether the variable cosubstrate was AdoMet or peptide. Data presented in Figure 6A show AdoMet as the variable substrate and WT-H3 as the fixed substrate. Figure 6B shows WT-H3 as the variable substrate and AdoMet as the fixed substrate in the reaction. The series of plots in both panels A and B of Figure 6 converged left of the *y*-axis and above or on the *x*-axis, suggesting neither AdoMet nor peptide binds to the enzyme in an ordered fashion. If AdoMet and peptide bind randomly and binding of one changes the dissociation constant of the other by a factor of α, there will be two binding constants for each substrate. The first corresponds to the enzyme−substrate binary complex (K_{ax}) and the other to the second substrate binding to make the ternary complex (αK_B), as shown in Figure 5A. From the slope and intercept of each plot on the *y*-axis ($1/V_{max}^{app}$), the preliminary kinetic constants were calculated (data not shown). Linear regression of $1/V_{max}^{app}$ values versus 1/[AdoMet] gave an αK_m^{AdoMet} value of 16.6 μM. Another analysis of slope values versus 1/[AdoMet] resulted in a K_m^{AdoMet} of 6 μM. A similar analysis and plots of $1/V_{max}^{app}$ versus 1/[WT-H3] or slope versus 1/[WT-H3] gave an αK_m^{WT-H3} and a K_m^{WT-H3} of 10 and 1.5 μM, respectively (data not shown).

Product Inhibition Studies of Recombinant SUV39H1 with AdoHcy and Trimethylated Peptide. The results thus far have suggested a random bi-bi reaction mechanism. To provide further evidence of this mechanism, product inhibition studies were performed. An equilibrium scheme for enzyme turnover in the presence or absence of an inhibitor is shown in Figure 7. Because of the structural relationship to the substrate, a product molecule of an enzymatic reaction is normally competitive with respect to the original substrate molecule. The product molecule may bind to the substrate-binding site of the enzyme or in the proximity of the substrate-binding site to exercise an inhibitory function via an enzyme−product complex. Thus, the amount of free enzyme available for the catalysis is dependent on the availability of the product in

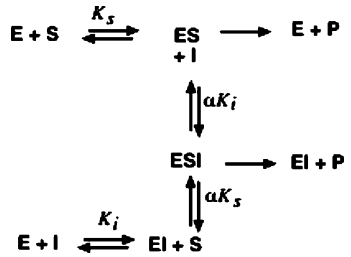

FIGURE 7: Enzyme turnover scheme for SUV39H1 in the presence or absence of inhibitor molecules. E (SUV39H1), S (AdoMet or unmethylated peptide), and I (AdoHcy or methylated peptide) are shown along with binary ES and EI complexes and the ternary ESI complex. The inhibition constant of the inhibitor is K_i for the enzyme and αK_i for the enzyme−substrate complex. K_S is the equilibrium constant for formation of the ES complex from the free enzyme and substrate. α is related to degree of modification the first substrate exerts on the binding of the second substrate.

Table 2: Product Inhibition Pattern of Recombinant SUV39H1[a]

product	variable substrate	fixed substrate	type of inhibition	K_i (μM)	αK_i (μM)
AdoHcy	AdoMet	peptide	competitive	12	
AdoHcy	peptide	AdoMet	mixed	38	9
Me-peptide	peptide	AdoMet	competitive	0.5	
Me-peptide	AdoMet	peptide	mixed	0.8	0.7

[a] The peptide used as the substrate was WT-H3. Me-peptide is trimethylated K9 and K27 peptide representing the fully methylated end product.

the reaction, and therefore, products in a reaction reduce the initial velocity. The free enzymes will turn over at the same rate as the reaction without product. That is why in a competitive mechanism of reaction the V_{max} remains the same and the K_m^{app} changes with inhibitor concentration. For a bisubstrate enzyme, a competitive inhibitor of one of the substrate binding sites will display either a competitive or mixed inhibition pattern, depending on which substrate is varied and which substrate binds first to the enzyme. Methyltransferases, such as SUV39H1, transfer a methyl group from AdoMet to Lys-9 of histone H3 generating two products, AdoHcy and methylated peptide. Varying the amount of AdoMet with different fixed amounts of AdoHcy yielded a nest of reciprocal plots that converged on the *y*-axis intercept (Figure 8A), suggesting AdoHcy is a competitive inhibitor of AdoMet. Nonlinear regression analysis of the series of curves yielded similar V_{max} values but different K_m^{app} values (data not shown). The K_i value for AdoHcy was determined by plotting K_m^{app} versus inhibitor concentration and was found to be 12 μM (Figure 8B). The K_i value for AdoHcy is almost identical to the K_m value for AdoMet (12 and 12.3 μM, respectively; Tables 2 and 3). Varying the amount of WT-H3 peptide with different fixed amounts of AdoHcy yielded a nest of reciprocal plots that converged beyond the *y*-axis, suggesting AdoHcy is a mixed inhibitor of peptide substrate (Figure 8C). By plotting the slope versus AdoHcy concentration (Figure 8D) and $1/V_{max}$ versus AdoHcy concentration (Figure 8E), we determined K_i and αK_i values of 9 and 38 μM, respectively, from the *y*-axis intercept as shown in Table 3.

Because of the inhibition pattern of AdoHcy being competitive with AdoMet and mixed with WT-H3 peptide, the mechanism of reaction may follow either a compulsory ordered or a random ordered mechanism. To distinguish the mechanism, product inhibition studies with methylated peptide was performed. Varying the amount of AdoMet with different fixed amounts of methylated peptide yielded a series of reciprocal plots that converged beyond the *y*-axis, suggesting the methylated peptide is a mixed inhibitor of the AdoMet substrate (Figure 8F). By plotting $1/V_{max}$ versus the methylated peptide concentration (Figure 8G) and the slope versus the methylated peptide concentration (Figure 8H), we determined K_i and αK_i values of 0.8 and 0.7 μM, respectively, from the *x*-axis intercept as shown in Table 2. A similar regression analysis was performed with varying amounts of WT-H3 with different fixed amounts of methylated peptide (Figure 8I). The reciprocal plots converged on the *y*-axis, suggesting a competitive inhibition pattern. Four sets of nonlinear regression curves yielded K_m^{app} values (data not shown). The K_i value of 0.5 μM for the methylated peptide was determined by plotting K_m^{app} values versus the methylated peptide concentration (Figure 8J). The pattern of product inhibition observed for recombinant SUV39H1 is summarized in Table 2. These results are consistent with a bi-bi random mechanism for SUV39H1 activity.

Steady-State Kinetic Properties of Recombinant SUV39H1 on Various Substrates. By studying an enzyme-catalyzed reaction at steady state, one can obtain essential kinetic parameters for a specific enzyme at a set of reaction conditions with a specific substrate. Since SUV39H1 can efficiently methylate K9 residues of histone H3 and synthetic peptides representing these sequences, both unmodified and modified peptides were used to study steady-state kinetic properties (Table 3). Variable amounts of either rH3, WT-H3, or WT-H3(dime) substrate with saturating amounts of AdoMet and a constant amount of recombinant SUV39H1 resulted in a hyperbolic curve fitted to eq 1. Representative

Table 3: Comparison of Steady-State Kinetic Parameters of SUV39H1 and Other Histone H3K9 Methyltransferases[a]

enzyme	substrate	k_{cat} (h^{-1})	K_m^{AdoMet} (μM)	K_m^{pep} (μM)	k_{cat}/K_m^{pep} ($\times 10^6$ M^{-1} h^{-1})	ref
SUV39H1	WT-H3	12 ± 0.5	12.3 ± 0.6	0.9 ± 0.1	13	this work
SUV39H1	WT-H3(K9-dime)	1.5 ± 0.1		0.07 ± 0.02	22	this work
SUV39H1	rH3	8 ± 0.8	6 ± 0.6	0.32 ± 0.07[b]	25[c]	this work
G9afl	WT-H3	88 ± 4	1.8 ± 0.2	0.9 ± 0.1	98	*36*
G9afl	WT-H3(K9-dime)	12 ± 3		2.3 ± 1.1	5.2	*36*
G9afl	rH3	46 ± 1	2.65 ± 0.2	0.3 ± 0.05[b]	153[c]	*36*
human SET9	rH3	14 ± 1	6.0 ± 1.4	5.4 ± 2.1	2.6	*24*
pea LSMT[d]	rubisco	137 ± 4	6.0 ± 1.3	1.4 ± 0.2	98	*26*
dSU(VAR)3-9	wt^{1-19}	396	25.9			*19*

[a] The peptide nomenclature is given in Materials and Methods. WT-H3 is the first 19 amino acids of the amino terminus of histone H3. WT-H3(K9-dm) is the dimethylated K9 peptide. Recombinant bacterially expressed human histone H3 is known as rH3. [b] Value for K_m^{H3}. [c] Value for k_{cat}/K_m^{H3}. [d] Pea LSMT is rubisco large subunit methyltransferase.

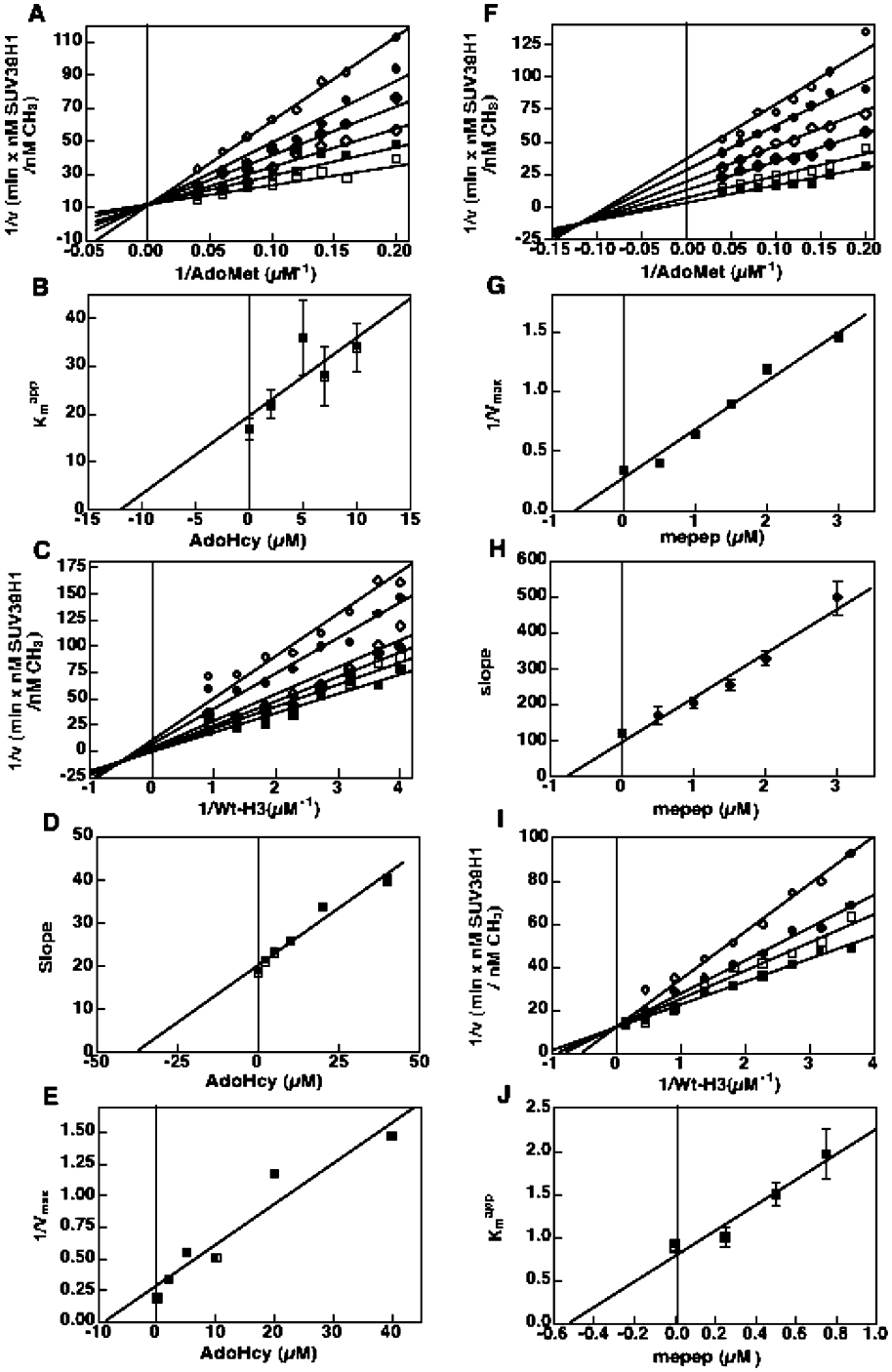

FIGURE 8: Product inhibition analysis of K9 methylation catalyzed by recombinant SUV39H1. (A) Double-reciprocal plot in the presence of a fixed concentration of AdoHcy: 0 (□), 2 (■), 5 (◇), 7 (◆), 10 (●), and 20 μM (○). The AdoMet concentration was variable (5, 6.25, 7.15, 8.35, 10, 12.5, 16.65, and 25 μM) in the reaction mixture. $1/v$ is plotted vs 1/[AdoMet] after linear regression. (B) Plots of K_m^{app} values obtained with nonlinear regression analysis of methylation values obtained in panel A were plotted against inhibitor AdoHcy concentration to determine K_i from the *x*-intercept. (C) As in panel A, a double-reciprocal plot in the presence of a fixed concentration of AdoHcy: 0 (■), 2 (□), 5 (◆), 10 (◇), 20 (●), and 40 μM (○). The unmethylated peptide concentration was variable (0.25, 0.275, 0.324, 0.367, 0.44, 0.55, 0.733, and 1.1 μM) in the reaction mixture. $1/v$ is plotted vs 1/[WT-H3] after linear regression. (D) Secondary plot for determination of inhibition constants for a mixed inhibitor. The value of K_i is determined from the *x*-intercept of a plot of the slope of the lines from the double-reciprocal plot in panel C as a function of inhibitor AdoHcy concentration. (E) Plot of $1/V_{max}$ vs AdoHcy concentration. The value of αK_i is determined from the *x*-intercept of the line. (F) As in panel C, a fixed increasing concentration of methylated peptide: 0 (■), 0.5 (□), 1 (◆), 1.5 (◇), 2 (●), and 3 μM (○) with a variable AdoMet substrate concentration (5, 6.25, 7.15, 8.35, 10, 12.5, 16.65, and 25 μM). $1/v$ is plotted vs 1/[AdoMet] after linear regression. (G) Secondary plot for determination of inhibition constants for a mixed inhibitor. The value of K_i is determined from the *x*-intercept of a plot of the slope of the lines from the double-reciprocal plot of panel F as a function of inhibitor methylated peptide concentration. (H) Plot of $1/V_{max}$ vs methylated peptide concentration. The value of αK_i is determined from the *x*-intercept of the line. (I) As in panel A, a double-reciprocal plot in the presence of a fixed concentration of the methylated peptide: 0 (■), 0.25 (□), 0.5 (●), and 0.75 μM (○). The unmethylated peptide concentration (0.275, 0.314, 0.367, 0.44, 0.55, 0.733, 1.1, 2.2, and 6.6 μM) was variable in the reaction mixture. $1/v$ is plotted vs 1/[WT-H3] after linear regression. (J) Secondary plot of K_m^{app} values obtained from nonlinear regression curve analysis [from methylated peptide (mepep) inhibition] vs mepep inhibitor concentration. The estimate of the K_i value is determined from the *x*-intercept.

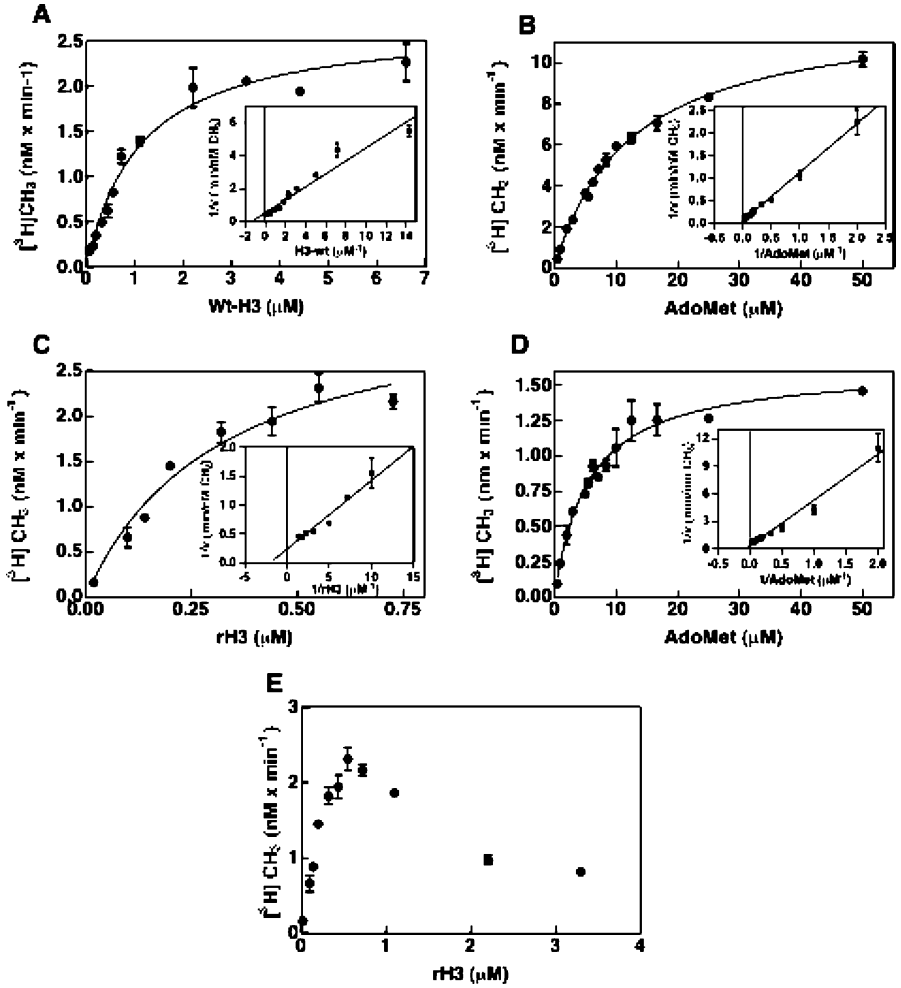

FIGURE 9: Representative substrate concentration−velocity curves and double-reciprocal plots of the initial velocity vs substrate concentration. (A) Full-length SUV39H1 activity with the WT-H3 peptide substrate. The methylation reaction was performed with substrate concentrations of 0.07, 0.14, 0.2, 0.32, 0.44, 0.55, 0.726, 1.1, 2.2, 3.3, 4.4, and 6.6 μM and fixed enzyme and AdoMet concentrations of 25 nM and 25 μM, respectively. The extent of product formation is plotted vs substrate concentration, and nonlinear regression was performed for determination of K_m^{pep} (K_m^{WT-H3}) values. The inset shows the Lineweaver−Burk plot of $1/v$ vs $1/s$. V_{max} and K_m^{WT-H3} were calculated from the substrate concentration−velocity plot. (B) Similar substrate concentration−velocity curve like that in panel A for a variable AdoMet concentration (2, 3, 5, 5.55, 6.25, 7.15, 8.35, 10, 12.5, 16.65, 25, and 50 μM), 25 nM SUV39H1, and 3.3 μM WT-H3. The extent of product formation is plotted vs substrate concentration, and nonlinear regression was performed for determination of K_m^{AdoMet} values. The Lineweaver−Burk plot of $1/v$ vs $1/s$ is shown in the inset. (C) Another similar substrate velocity curve like that in panel A, for a variable recombinant histone H3 concentration (0.02, 0.1, 0.14, 0.2, 0.32, 0.44, 0.55, and 0.726 μM), 25 nM SUV39H1, and 25 μM AdoMet. The extent of product formation is plotted vs substrate concentration, and nonlinear regression was performed for determination of K_m^{AdoMet} values. The Lineweaver−Burk plot of $1/v$ vs $1/s$ is shown in the inset. (D) Similar substrate velocity curve like that in panel B for a variable AdoMet concentration (1, 2, 3, 5, 5.55, 6.25, 7.15, 8.35, 10, 12.5, 16.65, 25, and 50 μM), 25 nM SUV39H1, and 0.6 μM recombinant human H3 molecules. The extent of product formation is plotted vs substrate concentration, and nonlinear regression was performed for determination of K_m^{AdoMet} values for rH3. The Lineweaver−Burk plot of $1/v$ vs $1/s$ is shown in the inset. (E) Methylation inhibition at higher concentrations of rH3. SUV39H1 (25 nM), AdoMet (25 μM), and various concentration of rH3 (0.02, 0.1, 0.14, 0.2, 0.32, 0.44, 0.55, 0.726, 1.1, 2.2, and 3.3 μM) were incubated for 30 min, and nanomolar concentration methyl group incorporation as a function of rH3 concentration is shown.

Michaelis−Menten plots for velocity as a function of WT-H3 (Figure 9A) and AdoMet concentration (Figure 9B) are shown. Methylation saturation was obtained above 1.0 μM substrate (Table 3). The kinetic parameters V_{max} and K_m were obtained after performing a nonlinear regression curve fit. From the V_{max}, the k_{cat} was calculated along with the enzyme's catalytic efficiency. Similar analyses were performed with rH3 substrate (Figure 9C, D) and WT-H3(dime) (data not shown). The kinetic constants are given in Table 3. The K_m values for WT-H3, WT-H3(dime), and rH3 were 0.9, 0.07, and 0.32 μM, respectively, demonstrating rH3 or WT-H3(dime) has a higher affinity for the enzyme. The WT-H3(dime) peptide displayed a poor turnover number (k_{cat}) of 1.5 h^{-1}, as compared to values of 12 and 8 h^{-1} for the unmethylated peptide and rH3 for SUV39H1, respectively, suggesting dimethylated K9 peptide as a relatively poor substrate of the enzyme. Surprisingly, we also observed rH3 concentration-dependent methylation inhibition above 0.55 μM substrate (Figure 9E).

Functional Role of the SUV39H1 Chromodomain in Catalysis. SUV39H1 is a modular protein with a distinctive chromodomain and a distinctive SET domain between amino acids 43 and 88 and amino acids 249 and 412, respectively. The chromodomains are conserved between different species (Figure 10A). The SET domain is involved in catalysis of histone Lys-9 methyltransferases since deletion or mutation of it impairs enzymatic activity (*7*, *23*). The chromodomain of SUV39H1 binds to H3K9 methylated histones (*45*). To

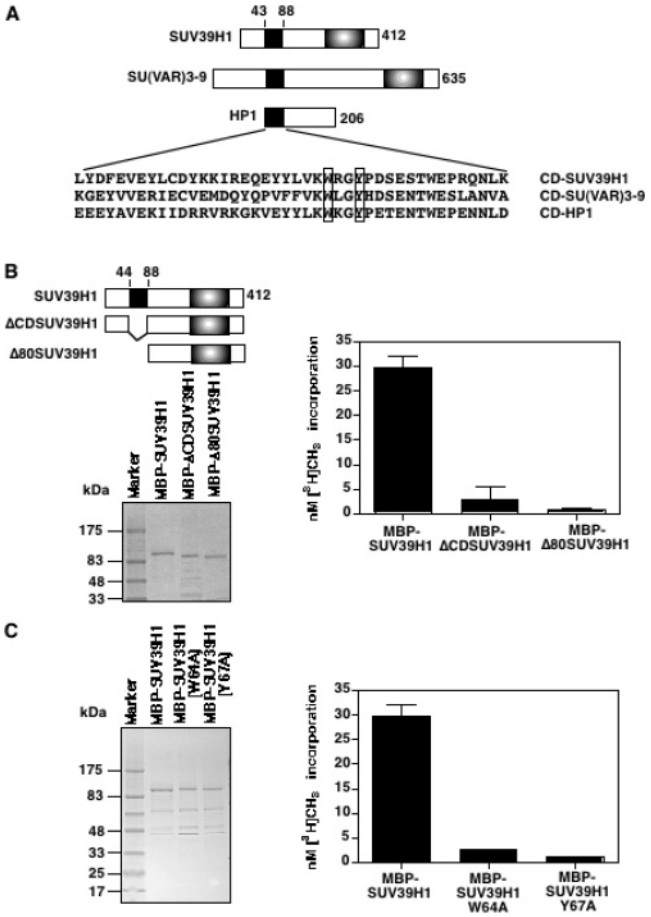

FIGURE 10: Involvement of the chromodomain in the SUV39H1-catalyzed methyltransferase reaction. (A) Schematic representation of the chromodomain containing human SUV39H1, *Drosophila* SU-(VAR)3-9, and heterochromatic protein HP1. The chromodomain (CD) is shown as a filled box, and below it, the amino acid residues for different CDs are aligned, as indicated at the right. Conserved amino acids W64 and Y67 are boxed. (B) A schematic diagram of full-length and deletion mutants is shown in the left panel. Purified MBP fusion SUV39H1 and deletion mutant fusions are shown below. A methyltransferase assay with 10 μM WT-H3, 50 nM enzymes, and 25 μM AdoMet was performed for 30 min, and the nanomolar concentration methyl group incorporation is shown at the right. (C) Like panel B, with the left panel showing the purified WT MBP−SUV39H1 fusion protein and point mutants MBP−SUV39H1(W64A) and MBP−SUV39H1(W67A). The activity assay of WT and point mutants is shown at the right. A methyltransferase assay was performed with 10 μM WT-H3, 100 nM enzymes, and 25 μM AdoMet. All assays in panels B and C were repeated in duplicate.

elucidate the function of the chromodomain, we generated the SUV39H1 deletion mutant lacking only the chromodomain (amino acids 43−81) or the first 80 amino acids of the N-terminus (Figure 10B). These proteins were expressed as MBP fusions, purified (Figure 10B), and assayed simultaneously along with the MBP full-length fusion using the WT-H3 substrate. Surprisingly, deletion of the chromodomain dramatically reduced enzymatic activity (Figure 10C), suggesting the chromodomain may play a significant role in enzymatic catalysis in coordination with the SET region. To identify specific amino acids that may be involved in catalysis, we mutated the conserved amino acids, W64A and Y67A (Figure 10D). These two amino acids are involved in forming an aromatic cage around methylated Lys-9 in the structure of HP1 (*46*). Indeed, MBP fusion mutant SUV39H1 (W64A or Y67A) methylated the WT-H3 substrate peptide much less efficiently than the WT fusion enzyme. Thus, both the chromodomain and the SET domain of SUV39H1 are important for catalysis.

DISCUSSION

Recombinant human SUV39H1 is catalytically active when expressed in a baculovirus expression system. The recombinant enzyme activity is facilitated at alkaline pH like that of the other Lys-9 methyltransferases such as DIM5 (*32*) and G9a (*36*). SUV39H1 did not use a peptide substrate constituting amino acids 1−13 (short peptide) of the histone amino termini but methylated well to a longer peptide comprising of the first 17 amino acids. However, the same short peptide was an excellent substrate of the G9a enzyme. These data show stringent substrate specificity for SUV39H1. The steady-state kinetic properties of the enzyme with rH3 or amino-terminal H3 peptide substrate showed a turnover number that is 7 times lower than that of G9a (Table 3). A similar lower catalytic efficiency was also observed with SUV39H1, suggesting G9a methylates the substrate better than SUV39H1 in vitro. However, the turnover numbers for *Drosophila* SU(VAR)3-9 were much higher compared to those of both human SUV39H1 and murine G9a. The K_m values for SUV39H1 and G9a were similar for rH3 and WT-H3, confirming both enzymes have similar binding properties for their substrates. The K_m^{AdoMet} values for G9a and SUV39H1 were strikingly different. While K_m^{AdoMet} values of G9a were between 2 and 3 μM, those of SUV39H1 were between 6 and 12 μM. The methylation reaction of SUV39H1 depended largely on AdoMet concentration (Figure 3A). The slope of the reaction progression curves increased with the amount of AdoMet. A similar AdoMet-dependent methyl transfer was observed for *Drosophila* SU(VAR)3-9 which had a K_m^{AdoMet} value of 25 μM (*35*). Thus, it may be possible that methylation of histone H3 may be regulated by the intracellular AdoMet concentration.

From the preincubation studies, it appears that the enzyme−AdoMet or −H3 peptide complex is catalytically active. This phenomenon is confirmed in inhibition studies with products, where the reaction for SUV39H1 follows a bi-bi random mechanism. Similar observations are made for other Lys-9 methyltransferases, G9a previously. Other methyltransferases such as human DNA (cytosine 5) methyltransferase 1 (*47*), M.HhaI (*48*), and M.BamHI (*49*) also have shown a similar random bi-bi mechanism. Preincubation studies show SUV39H1 can bind to either histone H3 or AdoMet (data not shown). Another SUV39H1 class of methyltransferases, DIM-5 of *N. crassa*, is shown to bind AdoHcy, in a large surface pocket, and this binding can be impaired via R155H, W161F, Y204F, and R238H mutations (*32*). In the product inhibition assay, we observed a competitive inhibition between AdoMet and AdoHcy and the K_i value was 12 μM, similar to the K_m value for AdoMet of 12.3 μM. This shows both AdoMet and AdoHcy have identical affinity for the substrate-binding site (Tables 2 and 3). A similar observation was made previously for euchromatic Lys-9 histone H3 methyltransferase, G9a (*36*). The fact that the K_i value for the methylated peptide versus unmethylated peptide was 0.5 μM for SUV39H1 and the fact that the K_m value for the unmethylated peptide remained ~0.9 μM suggest the methylated peptide has a higher affinity for the enzyme.

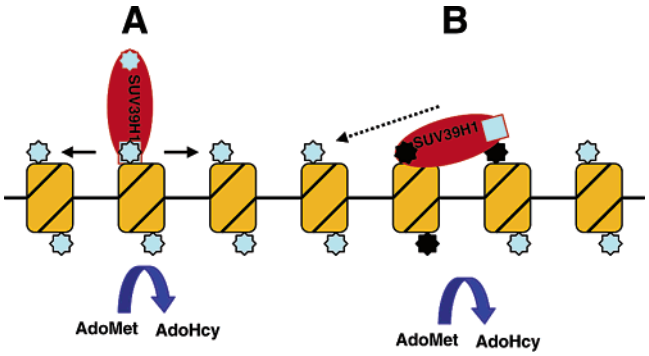

FIGURE 11: Model for catalysis of SUV39H1. (A) Methylation of unmethylated H3K9 (gray stars) via the catalytic SET domain (gray square) of SUV39H1 using cofactor AdoMet. (B) Methylated H3K9 (black stars) serves as an anchor for the chromodomain of SUV39H1. Following binding, the SET domain can methylate inter- and intranucleosomal unmethylated lysine 9 of histone H3.

However, these data may be interpreted with caution since the methylated peptide may bind to the chromodomain (*45*) and precipitate structural changes in the SET domain to impair the binding of the unmethylated peptide.

For human SUV39H1, a rH3 concentration of >0.55 μM inhibited the methylation reaction (Figure 9E). This inhibition was exclusive to rH3 but not with WT-H3 peptide representing the amino-terminal tail of histone H3. We have not observed any inhibition effect with WT-H3 up to 6.6 μM peptide (Figure 9A). The nonhyperbolic behavior of SUV39H1 may be attributed to product inhibition. With a typical product inhibition, at high substrate concentrations, the product exhibits a high affinity for the active site of the enzyme, to block the binding of the enzyme. If such a scenario were true, then both WT-H3 and rH3 would have exhibited the same kinetic behavior. Thus, the uniqueness of the rH3 substrate acting as an inhibitor suggests rH3 may bind to two different sites on the same enzyme or two different rH3 molecules may bind to the same enzyme at a higher concentration, thus making a rH3−SUV39H1−rH3 ternary complex that is essentially a dead-end complex. In this ternary complex, either one or both rH3 can be Lys-9 methylated rH3 molecule(s). This hypothesis of ternary complex formation gains support from the fact that SUV39H1 has a chromodomain and a catalytic SET domain embedded between amino acids 44 and 88 and amino acids 249 and 412, respectively, and the chromodomain is involved in chromatin binding in vivo. For instance, a fragment of SUV39H1 containing just the N-terminus and the chromodomain binds efficiently to heterochromatin when expressed in mammalian cells (*50*). Furthermore, fluorescence anisotropy experiments showed that the isolated chromodomain of SUV39H1 (like that of HP1; *51*) can specifically bind H3K9 trimethylated histone peptide with an affinity of 25 μM (*45*). Thus, it is possible for SUV39H1 to methylate the H3K9 tail using its catalytic domain and use the H3K9 methylated tail via binding of the chromodomain to methylate neighboring unmethylated H3 molecules (Figure 11). Alternatively, and consistent with the effect of chromodomain mutations on methylation of histone peptides, the binding of methyl-H3K9 to the chromodomain of SUV39H1 may regulate its activity via structural changes affecting the overall catalysis of the enzyme.

One of the similarities between *Drosophila* SU(VAR)3-9 and human SUV39H1 is that they both have a chromodomain preceding the SET domain. *Drosophila* SU(VAR)3-9 is ~635 amino acids long in contrast to the 412 amino acids in SUV39H1, and their amino terminus has very little identity. Deletion of 152 amino acids from *Drosophila* SU(VAR)3-9 resulted in a >90% loss of methyltransferase activity, and further deletion up to the chromodomain (279 amino acids) resulted in a catalytically inactive protein (*35*). Our experiments with human SUV39H1 without the first 81 amino acids or only the chromodomain deletion (amino acids 41−80) resulted in a major reduction of the methyltransferase activity in MBP−SUV39H1 fusions, suggesting that the chromodomain is important for enzymatic activity. W64A and Y67A point mutations, two conserved amino acids in the chromodomain, resulted in a catalytically impaired enzyme. Thus, this aromatic cage in SUV39H1 perhaps participates in recruitment and/or catalysis of Lys-9 methylation. Thus, the chromodomain of histone methyltransferases and other histone-modifying enzymes may play a significant role in the modulation of enzymatic catalysis.

ACKNOWLEDGMENT

We thank Dr. D. G. Comb for encouragement and New England Biolabs, Inc., for support and assistance.

REFERENCES

1. Luger, K., Mader, A. W., Richmond, R. K., Sargent, D. F., and Richmond, T. J. (1997) Crystal structure of the nucleosome core particle at 2.8 Å resolution, *Nature 389*, 251−260.
2. Van Holde, K. E. (1988) *Chromatin*, Springer-Verlag, New York.
3. Wolffe, A. P. (1998) *Chromatin Structure and Function*, 3rd ed., Academic Press, New York.
4. Mizzen, C. A., Yang, X. J., Kokubo, T., Brownell, J. E., Bannister, A. J., Owen-Hughes, T., Workman, J., Wang, L., Berger, S. L., Kouzarides, T., Nakatani, Y., and Allis, C. D. (1996) The TAF-(II)250 subunit of TFIID has histone acetyltransferase activity, *Cell 87*, 1261−1270.
5. Schiltz, R. L., Mizzen, C. A., Vassilev, A., Cook, R. G., Allis, C. D., and Nakatani, Y. (1999) Overlapping but distinct patterns of histone acetylation by the human coactivators p300 and PCAF within nucleosomal substrates, *J. Biol. Chem. 274*, 1189−1192.
6. Daujat, S., Bauer, U. M., Shah, V., Turner, B., Berger, S., and Kouzarides, T. (2002) Crosstalk between CARM1 methylation and CBP acetylation on histone H3, *Curr. Biol. 12*, 2090−2097.
7. Tachibana, M., Sugimoto, K., Fukushima, T., and Shinkai, Y. (2001) Set domain-containing protein, G9a, is a novel lysine-preferring mammalian histone methyltransferase with hyperactivity and specific selectivity to lysines 9 and 27 of histone H3, *J. Biol. Chem. 276*, 25309−25317.
8. Ogawa, H., Ishiguro, K., Gaubatz, S., Livingston, D. M., and Nakatani Y. (2002) A complex with chromatin modifiers that occupies E2F- and Myc-responsive genes in G0 cells, *Science 296*, 1132−1136.
9. Yang, L., Xia, L., Wu, D. Y., Wang, H., Chansky, H. A., Schubach, W. H., Hickstein, D. D., and Zhang, Y. (2002) Molecular cloning of ESET, a novel histone H3-specific methyltransferase that interacts with ERG transcription factor, *Oncogene 21*, 148−152.
10. Lo, W. S., Duggan, L., Emre, N. C., Belotserkovskya, R., Lane, W. S., Shiekhattar, R., and Berger, S. L. (2001) Snf1: A histone kinase that works in concert with the histone acetyltransferase Gcn5 to regulate transcription, *Science 293*, 1142−1146.
11. Wei, Y., Yu, L., Bowen, J., Gorovsky, M. A., and Allis, C. D. (1999) Phosphorylation of histone H3 is required for proper chromosome condensation and segregation, *Cell 97*, 99−109.
12. De Souza, C. P., Osmani, A. H., Wu, L. P., Spotts, J. L., and Osmani, S. A. (2000) Mitotic histone H3 phosphorylation by the NIMA kinase in *Aspergillus nidulans*, *Cell 102*, 293−302.

13. Santos-Rosa, H., Schneider, R., Bannister, A. J., Sherriff, J., Bernstein, B. E., Emre, N. C., Schreiber, S. L., Mellor, J., and Kouzarides, T. (2002) Active genes are tri-methylated at K4 of histone H3, *Nature 419*, 407−411.
14. Bernstein, B. E., Kamal, M., Lindblad-Toh, K., Bekiranov, S., Bailey, D. K., Huebert, D. J., McMahon, S., Karlsson, E. K., Kulbokas, E. J., III, Gingeras, T. R., Schreiber, S. L., and Lander, E. S. (2005) Genomic maps and comparative analysis of histone modifications in human and mouse, *Cell 120*, 169−181.
15. Roopra, A., Qazi, R., Schoenike, B., Daley, T. J., and Morrison, J. F. (2004) Localized domains of G9a-mediated histone methylation are required for silencing of neuronal genes, *Mol. Cell 14*, 727−738.
16. Gyory, I., Wu, J., Fejer, G., Seto, E., and Wright, K. L (2004) PRDI-BF1 recruits the histone H3 methyltransferase G9a in transcriptional silencing, *Nat. Immunol. 5*, 299−308.
17. Avner, P. and Heard, E. (2001) X-chromosome inactivation: Counting, choice and initiation, *Nat. Rev. Genet. 2*, 59−67.
18. Heard, E., Rougeulle, C., Arnaud, D., Avner, P., Allis, C. D., and Spector, D. L. (2001) Methylation of histone H3 at Lys-9 is an early mark on the X chromosome during X inactivation, *Cell 107*, 727−738.
19. Brehm, A., Tufteland, K. R., Aasland, R., and Becker, P. B. (2004) The many colours of chromodomains, *BioEssays 26*, 133−140.
20. Koonin, E. V., Zhou, S., and Lucchesi, J. C. (1995) The chromo superfamily: New members, duplication of the chromodomain and possible role in delivering transcription regulators to chromatin, *Nucleic Acids Res. 23*, 4229−4233.
21. Yeates, T. O. (2002) Structures of SET domain proteins: Protein lysine methyltransferases make their mark, *Cell 111*, 5−7.
22. Jacobs, S. A., Harp, J. M., Devarakonda, S., Kim, Y., Rastinejad, F., and Khorasanizadeh, S. (2002) The active site of the SET domain is constructed on a knot, *Nat. Struct. Biol. 9*, 833−888.
23. Rea, S., Eisenhaber, F., O'Carroll, D., Strahl, B. D., Sun, Z. W., Schmid, M., Opravil, S., Mechtler, K., Ponting, C. P., Allis, C. D., and Jenuwein, T. (2000) Regulation of chromatin structure by site-specific histone H3 methyltransferases, *Nature 406*, 593−599.
24. Tachibana, M., Sugimoto, K., Nozaki, M., Ueda, J., Ohta, T., Ohki, M., Fukuda, M., Takeda, N., Niida, H., Kato, H., and Shinkai, Y. (2002) G9a histone methyltransferase plays a dominant role in euchromatic histone H3 lysine 9 methylation and is essential for early embryogenesis, *Genes Dev. 16*, 1779−1791.
25. Czermin, B., Schotta, G., Hulsmann, B. B., Brehm, A., Becker, P. B., Reuter, G., and Imhof, A. (2001). Physical and functional association of SU(VAR)3-9 and HDAC1 in *Drosophila*, *EMBO Rep. 2*, 915−919.
26. Bannister, A. J., Zegerman, P., Partridge, J. F., Miska, E. A., Thomas, J. O., Allshire, R. C., and Kouzarides, T. (2001) Selective recognition of methylated lysine 9 on histone H3 by the HP1 chromodomain, *Nature 410*, 120−124.
27. Fischle, W., Wang, Y., Jacobs, S. A., Kim, Y., Allis, C. D., and Khorasanizadeh, S. (2003) Molecular basis for the discrimination of repressive methyl-lysine marks in histone H3 by Polycomb and HP1 chromodomains, *Genes Dev. 17*, 1870−1881.
28. Rice, J. C., Briggs, S. D., Ueberheide, B., Barber, C. M., Shabanowitz, J., Hunt, D. F., Shinkai, Y., and Allis, C. D. (2003) Histone methyltransferases direct different degrees of methylation to define distinct chromatin domains, *Mol. Cell 12*, 1591−1598.
29. Peters, A. H., Kubicek, S., Mechtler, K., O'Sullivan, R. J., Derijck, A. A., Perez-Burgos, L., Kohlmaier, A., Opravil, S., Tachibana, M., Shinkai, Y., Martens, J. H., and Jenuwein, T. (2003) Partitioning and plasticity of repressive histone methylation states in mammalian chromatin, *Mol. Cell 12*, 1577−1589.
30. Peters, A. H., O'Carroll, D., Scherthan, H., Mechtler, K., Sauer, S., Schofer, C., Weipoltshammer, K., Pagani, M., Lachner, M., Kohlmaier, A., Opravil, S., Doyle, M., Sibilia, M., and Jenuwein, T. (2001) Loss of the Suv39h histone methyltransferases impairs mammalian heterochromatin and genome stability, *Cell 107*, 323−337.
31. Zhang, X., Tamaru, H., Khan, S. I., Horton, J. R., Keefe, L. J., Selker, E. U., and Cheng, X. (2002) Structure of the *Neurospora* SET domain protein DIM-5, a histone H3 lysine methyltransferase, *Cell 111*, 117−127.
32. Zhang, X., Yang, Z., Khan, S. I., Horton, J. R., Tamaru, H., Selker, E. U., and Cheng, X. (2003) Structural basis for the product specificity of histone lysine methyltransferases, *Mol. Cell 12*, 177−185.
33. Xiao, B., Jing, C., Wilson, J. R., Walker, P. A., Vasisht, N., Kelly, G., Howell, S., Taylor, I. A., Blackburn, G. M., and Gamblin, S. J. (2003) Structure and catalytic mechanism of the human histone methyltransferase SET7/9, *Nature 421*, 652−656.
34. Wilson, J. R., Jing, C., Walker, P. A., Martin, S. R., Howell, S. A., Blackburn, G. M., Gamblin, S. J., and Xiao, B. (2002) Crystal structure and functional analysis of the histone methyltransferase SET7/9, *Cell 111*, 105−115.
35. Eskeland, R., Czermin, B., Boeke, J., Bonaldi, T., Regula, J. T., and Imhof, A. (2004) The N-terminus of *Drosophila* SU(VAR)3-9 mediates dimerization and regulates its methyltransferase activity, *Biochemistry 43*, 3740−3749.
36. Patnaik, D., Chin, H. G., Esteve, P. O., Benner, J., Jacobsen, S. E., and Pradhan, S. (2004) Substrate specificity and kinetic mechanism of mammalian G9a histone H3 methyltransferase, *J. Biol. Chem. 279*, 53248−53258.
37. Trievel, R. C., Beach, B. M., Dirk, L. M., Houtz, R. L., and Hurley, J. H. (2002) Structure and catalytic mechanism of a SET domain protein methyltransferase, *Cell 111*, 91−103.
38. Kwon, T., Chang, J. H., Kwak, E., Lee, C. W., Joachimiak, A., Kim, Y. C., Lee, J., and Cho, Y. (2003) Mechanism of histone lysine methyl transfer revealed by the structure of SET7/9-AdoMet, *EMBO J. 22*, 292−303.
39. Manzur, K. L., Farooq, A., Zeng, L., Plotnikova, O., Koch, A. W., Sachchidan, and Zhou, M. M. (2003) A dimeric viral SET domain methyltransferase specific to Lys27 of histone H3, *Nat. Struct. Biol. 10*, 187−196.
40. Tachibana, M., Ueda, J., Fukuda, M., Takeda, N., Ohta, T., Iwanari, H., Sakihama, T., Kodama, T., Hamakubo, T., and Shinkai, Y. (2005) Histone methyltransferases G9a and GLP form heteromeric complexes and are both crucial for methylation of euchromatin at H3K9, *Genes Dev. 19*, 815−826.
41. Collins, R. E., Tachibana, M., Tamaru, H., Smith, K. M., Jia, D., Zhang, X., Selker, E. U., Shinkai, Y., and Cheng, X. (2005) In vitro and in vivo analyses of a Phe/Tyr switch controlling product specificity of histone lysine methyltransferases, *J. Biol. Chem. 280*, 5563−5570.
42. O'Reilly, D. R., Miller, L. K., and Luckow, V. A. (1992) in *Baculovirus Expression Vectors: A Laboratory Manual*, pp 124−127, W. H. Freeman and Co., New York.
43. Segal, I. H. (1975) *Enzyme kinetics: Behavior and analysis of rapid equilibrium and steady-state enzyme systems*, John Wiley and Sons, Inc., New York.
44. Stewart, M. D., Li, J., and Wong, J. (2005) Relationship between histone H3 lysine 9 methylation, transcription repression, and heterochromatin protein 1 recruitment, *Mol. Cell. Biol. 25*, 2525−2538.
45. Jacobs, S. A., Fischle, W., and Khorasanizadeh, S. (2004) Assays for the determination of structure and dynamics of the interaction of the chromodomain with histone peptides, *Methods Enzymol. 376*, 131−148.
46. Jacobs, S. A., and Khorasanizadeh, S. (2002) Structure of HP1 chromodomain bound to a lysine 9-methylated histone H3 tail, *Science 295*, 2080−2083.
47. Bacolla, A., Pradhan, S., Roberts, R. J., and Wells, R. D. (1999) Recombinant human DNA (cytosine-5) methyltransferase. I. Expression, purification, and comparison of de novo and maintenance methylation, *J. Biol. Chem. 274*, 33011−33019.
48. Vilkaitis, G., Merkiene, E., Serva, S., Weinhold, E., and Klimasauskas, S. (2001) The mechanism of DNA cytosine-5 methylation. Kinetic and mutational dissection of Hhal methyltransferase, *J. Biol. Chem. 276*, 20924−20934.
49. Malygin, E. G., Zinoviev, V. V., Evdokimov, A. A., Lindstrom, W. M., Jr., Reich, N. O., and Hattman, S. (2003) DNA (cytosine-N4-)- and -(adenine-N6-)-methyltransferases have different kinetic mechanisms but the same reaction route. A comparison of M.BamHI and T4 Dam, *J. Biol. Chem. 278*, 15713−15719.
50. Melcher, M., Schmid, M., Aagaard, L., Selenko, P., Laible, G., and Jenuwein, T. (2000) Structure−function analysis of SUV39H1 reveals a dominant role in heterochromatin organization, chromosome segregation, and mitotic progression, *Mol. Cell. Biol. 20*, 3728−3741.
51. Jacobs, S. A., Taverna, S. D., Zhang, Y., Briggs, S. D., Li, J., Eissenberg, J. C., Allis, C. D., and Khorasanizadeh, S. (2001) Specificity of the HP1 chromodomain for the methylated N-terminus of histone H3, *EMBO J. 20*, 5232−5241.

BI051997R